

Alternative High Occupancy/Toll Lane Pricing Strategies and their Effect on Market Share

Michael Janson and David Levinson

High Occupancy/Toll (HOT) Lanes typically charge a varying toll to single occupant vehicles (SOVs), with the toll increasing during more congested periods. The toll is usually tied to time of day or to the density of vehicles in the HOT lane. The purpose of raising the toll with congestion is to discourage demand enough to maintain a high level of service (LOS) in the HOT lane. [Janson and Levinson \(2014\)](#) demonstrated that the HOT toll may act as a signal of downstream congestion (in both general purpose (GP) and HOT lanes), causing an increase in demand for the HOT lane, at least at lower prices. This paper builds off that research and explores alternative HOT lane pricing strategies, including the use of GP density as a factor in price to more accurately reflect the value of the HOT lane. In addition, the paper explores the potential effect these strategies would have on the HOT lane vehicle share through a partial equilibrium analysis. This analysis demonstrates the change in demand elasticity with price, showing the point at which drivers switch from a positive to negative elasticity.

Total Words = 4423 + 250*12(6 Figures & 6 Tables) = 7423

1 Introduction

High Occupancy/Toll (HOT) lanes charge a toll to single occupant vehicles (SOVs) for several reasons. The toll serves to raise revenue to cover operating costs and to regulate the demand of SOVs. HOT lanes around the country use different methods for determining the toll, however, all methods raise the toll price during more congested periods. The theory is, a higher toll price discourages demand and is used to maintain a high level of service (LOS) in the HOT lane(s). Janson and Levinson (2014) showed, however, that a higher price may act as a signal of downstream congestion (in both the general purpose (GP) and HOT lanes), causing demand for the HOT lane to increase to a point.

This paper explores current HOT pricing strategies and proposes some alternatives. These alternative strategies are tested using a partial equilibrium analysis. This analysis uses a calibrated HOT lane choice model to determine the HOT lane share at various prices and determine demand elasticity to price.

2 Pricing on HOT Lanes

Table 1 summarizes the tolling strategies of various HOT lanes around the United States. Several HOT lane systems base the toll on time of day, while others are dependent on HOT density or speed. Details of Minneapolis' MnPASS lanes' pricing system are outlined in the following section.

Table 1: HOT Lane Tolling Strategies

City	Highway	System Open Date	Length (miles)	Toll Dependency
Atlanta ⁷	I-85	2011	16	HOT Density
Denver ⁴	I-25	2006	7	Time of Day
Houston ⁹	I-10	2009	12	Time of Day
Miami ⁶	I-95	2008, 2014	8, 13 (total)	HOT Density
Minneapolis ¹⁰	I-394	2005	11	HOT Density
Orange County ¹	SR 91	2003	10	Time of Day
San Diego ⁵	I-15	1998	12	HOT Density
Seattle ¹³	SR 167	2008	9	HOT Speed
Washington, D.C. ¹²	I-495	2012	14	HOT Density

3 MnPASS Current Operation

The MnPASS lanes in Minneapolis operate during the morning and afternoon peak periods. With several exceptions, the general operating hours are from 6:00-10:00 and 14:00-19:00. Prices during operation times range from a minimum of \$0.25 to a maximum \$8.00. I-394 and I-35W are each divided into multiple sections with prices posted for use of each segment. The maximum price

23 applies to use of each section individually, as well as use of all sections.

24 Prices are adjusted every three minutes based on density levels measured in the MnPASS lanes
 25 only. Traffic levels in the general purpose (GP) lanes do not directly influence price. Loop detector
 26 counts are taken every 30 seconds and used to calculate the density in the MnPASS lanes plazas
 27 along the corridor. Density measurements are averaged over the last 6 minute period in order
 28 to smooth out fluctuations and based only on downstream congestion. Price is dictated by the
 29 magnitude of density as well as the change in density over the previous 6 minutes. A rise in density
 30 creates an increase in price. Table 2 displays the pricing plan, which regulates the price based
 31 on density level. Minimums and maximums for a given LOS must be maintained. The table also
 32 indicates the changes in price caused by a change in density.

Table 2: Pricing Plan for Normal Operation of MnPASS Lanes (both I-35W and I-394)

Level of Service	Min K	Max K	Min Rate (\$)	Default Rate (\$)	Max Rate (\$)
A	0	11	0.25	0.25	0.50
B	12	18	0.50	0.50	1.50
C	19	31	1.50	1.50	2.50
D	32	42	2.50	3.00	3.50
E	43	49	3.50	5.00	5.00
F	50	50	5.00	8.00	8.00

Change in Price from Density Change						
K	$\Delta 1$	$\Delta 2$	$\Delta 3$	$\Delta 4$	$\Delta 5$	$\Delta 6$
0-18	0.25	0.25	0.25	0.25	0.25	0.25
19+	0.25	0.50	0.75	1.00	1.25	1.50

Density in veh/mi/ln; Prices in \$

33 4 Alternative Pricing Strategies

34 The following pricing strategies are proposed alternatives to the current system used on the Mn-
 35 PASS HOT lanes. The continuous function is similar to the current pricing algorithm in that it
 36 relies strictly on HOT density for determining price, however, instead of relying on a series of
 37 tables, price is determined from a simple mathematical equation. The three other value pricing
 38 strategies incorporate GP density and use the difference in density between the HOT and GP lanes
 39 to determine price. Details of the pricing strategies are outlined below.

40 In all cases, the prices are confined to several constraints to match the existing pricing algorithm.
 41 The minimum price is \$0.25, the maximum \$8.00 and all prices are rounded to the nearest \$0.25.
 42 The following equation represents the constraints which are applied after the unconstrained price is
 43 determined.

$$P_{constrained} = Rnd(\text{Min}(\text{Max}(P_{unconstrained}, 0.25), 8.00), 0.25) \quad (1)$$

44 $P_{unconstrained}$ may be defined several ways, as discussed below.

45 4.1 Continuous Function

46 Prices using this function are determined by:

$$P_{continuous} = \alpha * K_{HOT}^{\beta} \quad (2)$$

47 where P represents the price in USD and K the density in vehicles/mile/lane.

48 K_{HOT} is found using the same method as the current algorithm (maximum downstream density
49 averaged over last 6 minutes). α and β are constants which can be adjusted to achieve the desired
50 curve.

51 4.2 Unweighted Value Pricing

52 While the current pricing algorithm only evaluates the density in the HOT lane, this pricing strat-
53 egy would compute price based on the difference in density between the GP and HOT lanes. The
54 difference in density between the lane groups is correlated with a difference in time savings and
55 therefore, the value provided by the HOT lane. Implementation of this pricing scheme (and sub-
56 sequent strategies), will require the integration of GP density as a factor in determining price. GP
57 density is averaged among parallel detectors. The maximum downstream GP density is then used
58 to determine price, along with the maximum downstream HOT density.

$$P_{Value_{unweighted}} = \gamma * [K_{GP} - K_{HOT}] \quad (3)$$

59 4.3 $HOT_{weighted}$ Value Pricing

60 Differences in density between GP and HOT lanes do not correlate directly to travel speeds. Rather,
61 there is a correlation with the magnitude of densities. For example, little speed difference exists
62 between 10 and 20 vehicles/mi/ln (approximately 6 and 12 veh/km/ln), both likely experience free
63 flow speeds. However, a greater speed difference exists at higher densities (between 40 and 50
64 veh/mi/ln (approximately 25 and 31 veh/km/ln)). Therefore, it makes more sense to weight the
65 density difference between the GP and HOT, based on the magnitude of density. This function
66 weights the difference based on the magnitude of the HOT lane density. Similarly to the current
67 algorithm, price will increase proportionally with HOT density.

$$P_{Value_{HOT_{weighted}}} = \delta * [K_{GP} - K_{HOT}] * K_{HOT} \quad (4)$$

68 4.4 $GP_{weighted}$ Value Pricing

69 This pricing strategy is weighted based on GP density instead of HOT density. If K_{GP} is much
70 greater than K_{HOT} and K_{HOT} is very low, then the HOT weighted value pricing strategy would
71 yield a low price even though there would be a significant value in using the HOT lane. By weighting
72 based on K_{GP} , this strategy ties price more directly to the GP lane congestion and the actual time
73 savings gained by using the HOT lane.

$$P_{ValueGP_{weighted}} = \sigma * [K_{GP} - K_{HOT}] * K_{GP} \quad (5)$$

74 5 Partial Equilibrium Analysis

75 The partial equilibrium analysis involves using a fixed demand of SOVs with predefined commute
76 times and locations to calibrate a lane choice model and eventually test alternative pricing strate-
77 gies. The SOVs are equipped with transponders and can decide whether to use the MnPASS or
78 GP lanes based on the toll and their expected travel time and reliability. The following sections
79 outline the process.

80 6 Lane Choice Model

81 This HOT lane choice model extends work done by Carlos Carrion ([Carrion, 2010](#)). The binomial
82 logit model determines the probability of a vehicle using the HOT lane based on several independent
83 variables. These variables include estimated travel times and travel time variability for both the
84 HOT lane and the GP lanes, as well as the posted toll price. The lane choice model applies only
85 to SOVs equipped with transponders. SOVs not equipped with transponders are not allowed to
86 use the MnPASS lanes. A separate subscription choice model was developed to determine which
87 vehicles are equipped with transponders. Details of this model are outlined in [Owen et al. \(2013\)](#).

88 6.1 Model Coefficients

89 Utility from [Carrion \(2010\)](#) is described as:

$$U = f(T, V, P, A)$$

90 where:

91 T: Expected Travel Time The utility decreases with an increase in expected travel time, decreasing
92 the probability of using the given lane type. Expected travel time is measured in minutes.

93 V: Travel Time Variability Travel time variability in this model is defined as the 90th percentile -
94 50th percentile to correspond with Carrion (2010). This value is calculated separately for the HOT
95 lane and GP lanes. Like expected travel time, an increase in variability decreases the probability
96 of using that lane. Travel time variability is measured in minutes.

97 P: Expected Toll Price The expected toll variable is based on the dynamic message sign posted
98 price. The price corresponds to a user's entry and exit points. This model assumes all drivers will
99 exit in downtown Minneapolis. Therefore, the expected toll will vary only by entry point. Toll
100 prices are in USD. The negative sign indicates a dissuasion from higher tolls, assuming all other
101 factors remain constant.

102 A: Alternative Specific Constant In this model, the ASC was defaulted to zero and adjusted if
103 necessary in the calibration.

104 7 Calibration of Lane Choice Model

105 While the model was previously calibrated in (Carrion, 2010), the calibration relied on a very small
106 sample size of vehicles and was therefore, recalibrated using the following methodology.

107 The lane choice model was calibrated by matching a set of simulated vehicles' HOT lane decisions
108 to historical data. The list of vehicles was generated from trip tables provided by the Metropolitan
109 Council. All vehicles are SOVs traveling eastbound to downtown Minneapolis on I-394 between 6:00-
110 10:00 AM. Each vehicle has an entrance ramp and time of entry into the system. The subscription
111 choice model from Owen et al. (2013) is first applied to filter non-transponder owning SOVs. Each
112 vehicle experiences various travel times based on the entrance ramp and time of entry. These travel
113 times are the basis of the expected travel time and travel time reliability parameters of the lane
114 choice model. Details of the calibration steps are outlined in the following sections.

115 The lane choice model coefficients are adjusted using a grid search technique. Default values for the
116 coefficients were taken from Carrion (2010), with the exception of the alternative specific constant
117 (ASC) which was set to zero. The grid search approach involves adjusting each of the coefficients
118 separately, while keeping all others constant. The first coefficient is altered until the model achieves
119 its best fit to the calibration target. This coefficient is then kept constant and the second coefficient
120 is adjusted and so on until the fit can no longer be improved.

121 In this model, the ratio of expected travel time to travel time variability was kept constant and
122 the ASC was defaulted to zero. The travel time coefficients were adjusted first, followed by the
123 toll coefficient and ASC (if necessary). The ratio of expected travel time to travel time variability
124 was kept constant due to the extensive literature research outlined in from Carrion and Levinson
125 (2012) in determining this value.

126 7.1 Travel History

127 Each vehicle builds a travel time history by experiencing MnPASS travel times along the corridor
128 based on their entrance ramp and time of entry. All travel is along I-394 Eastbound to downtown
129 Minneapolis. The travel times are calculated using loop detector data from each Wednesday of
130 2012 (except July 4 and December 26). This travel history determines a vehicle's expected travel
131 time (mean of travel history) and travel time variability (90th percentile minus 50th percentile).

132 7.2 Calibration Target

133 In order to calibrate the lane choice model, it is necessary to determine the probability that a
134 transponder owning SOV will use the MnPASS lane.

135 Using Bayes' theorem:

$$Pr(L|R) = Pr(R|L) * Pr(L)/Pr(R) \quad (6)$$

136 $Pr(R)$ is the probability of radio transponder ownership (from subscription choice model). $Pr(L)$
137 represents the probability of using the HOT lane among all SOVs. $Pr(R|L)$ is the probability of
138 owning a transponder given use of the HOT lane. Since only SOVs are being considered, $Pr(R|L)$
139 is 1 (or 100%) assuming no illegal use of the HOT lane.

140 $Pr(L)$ was calculated by finding the number of SOVs using the MnPASS lane and dividing by
141 total number of vehicles using the corridor during the same time period. Total vehicle counts were
142 gathered from loop detector data. The number of HOVs using the GP lanes is assumed to be zero.
143 Counts of SOVs using the MnPASS lane come from transponder data which shows entry and exit
144 plazas and entry time, along with paid toll price. By comparing the counts throughout morning
145 peak period with the GP loop detector data, $Pr(L)$ can be determined.

146 $Pr(R)$ was calculated by correlating the subscription choice model in [Owen et al. \(2013\)](#) with
147 subscription data for each transportation analysis zone (TAZ) along the corridor. Each vehicle's
148 entrance ramp can be probabilistically correlated to surrounding TAZs. By then applying the
149 subscription choice model to the total set of SOVs, a subset of transponder equipped SOVs is
150 formed. This is likely a lower bound of transponder usage, since transponder owners in a TAZ are
151 more likely to use MnPASS (or MnPASS corridor users are more likely to own a transponder) than
152 a random traveler from a TAZ.

153 7.3 Calibration Day

154 In previous research conducted by the Minnesota Traffic Observatory (MTO), trip generation mod-
155 els and traffic simulations were calibrated to November 29, 2011. This day was selected because it
156 was an average day with no weather or crash related problems along the MnPASS corridors. Due

157 to the connection of this research to the calibrated simulation used in the MTO, this calendar day
 158 was selected for calibration of the lane choice model.

159 The $Pr(L)$ value from 11/29/2011 and $Pr(R)$, result in:

$$Pr(L|R) = (100\%) * (11.8\%)/(17.3\%) = 68.1\% \quad (7)$$

160 7.4 Price-Time Savings and Price-Reliability Models

161 Although the MnPASS toll price fluctuates based on HOT density, there is a direct correlation
 162 between the toll and the time savings the MnPASS lanes provide over the GP lanes. The higher
 163 the toll, the greater the time savings. This correlation is observed by users and explains the positive
 164 demand elasticity to price results in [Janson and Levinson \(2014\)](#).

165 Using average toll prices and time savings data from 2012, a log relationship was fit. The bimodal
 166 relationship of the data meant two log functions were fit, one for congestion onset and one for the
 167 offset.

168 The relationship between price and time savings during congestion onset and offset are displayed
 169 in [Table 3](#). The corresponding curves are displayed in [Figure 1](#).

170 The increased travel time reliability of the MnPASS lanes is also proportional to the toll price.
 171 Again, two log functions were fit to the congestion onset and offset data.

172 The relationship between price and time savings during congestion onset and offset are displayed
 173 in [Table 3](#). The corresponding curves are displayed in [Figure 2](#).

Table 3: Price-Time Savings and Price-Reliability Regression Results

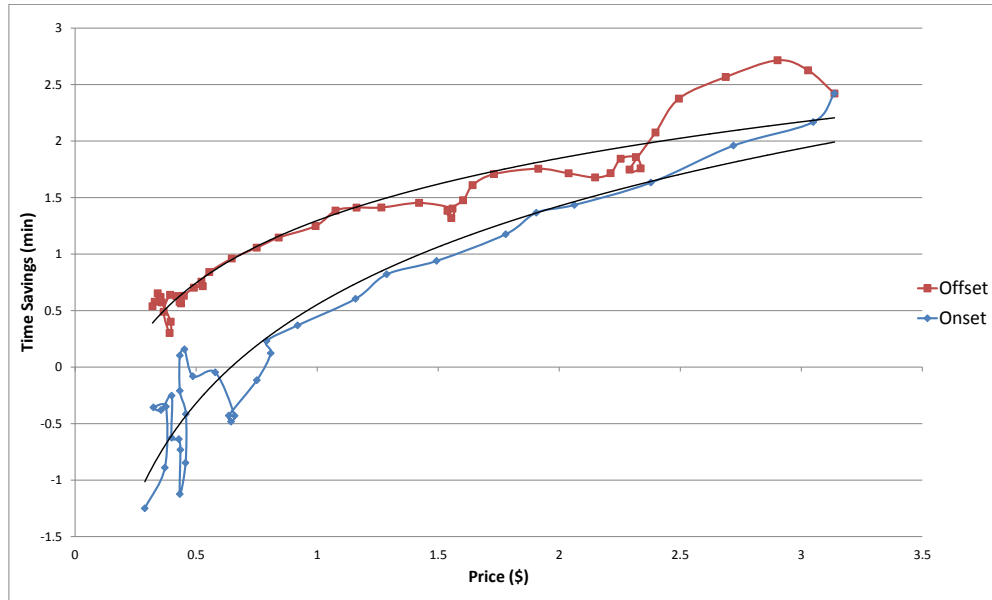
Variable	Time Savings vs Price		Time Variance Difference vs Price	
	Onset	Offset	Onset	Offset
Intercept	0.5527(0.05972)***	1.2965(0.02912)***	0.9566(0.03867)***	1.6636(0.01664)***
$\log(P)$	1.2587(0.07732)***	0.7953(0.03743)***	1.1413(0.05006)***	0.926(0.02139)***
n	40	40	40	40
r^2	0.8923	0.913	0.942	0.9657

(Standard error in parentheses)

Significance * 0.05, ** 0.01, *** 0.001

Time Savings and Time Variance Difference in minutes are the dependent variables, price in USD is the independent variable

Figure 1: Price-Time Savings Log Model

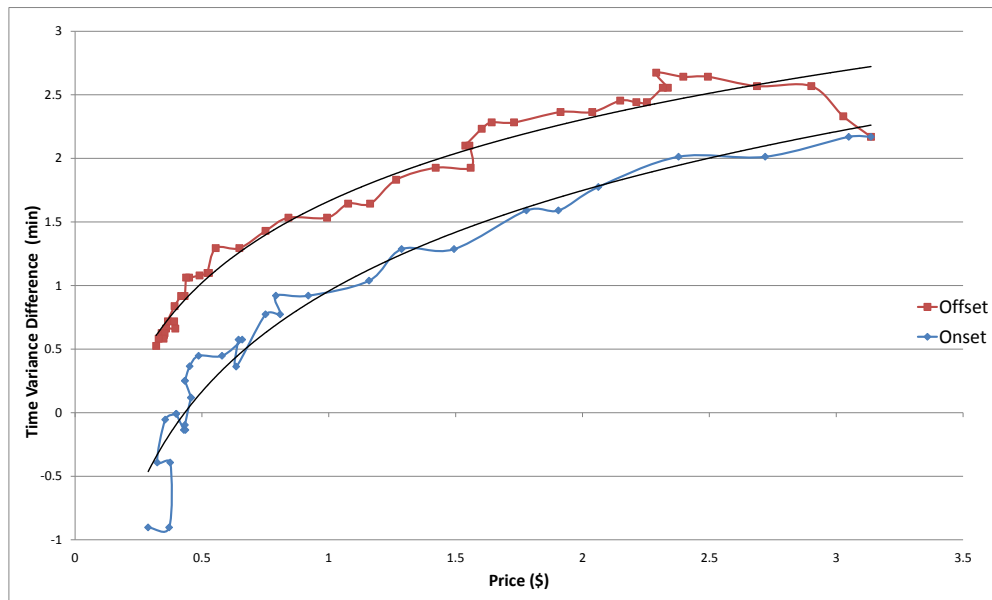


$$\Delta T_{onset} = 1.2587 \ln(P) + 0.5527 \quad (r^2 = 0.8923)$$

$$\Delta T_{offset} = 0.7953 \ln(P) + 1.2965 \quad (r^2 = 0.913)$$

where ΔT is travel time savings in minutes and P is price in USD

Figure 2: Price-Reliability Model



$$\Delta V_{onset} = 1.1413 \ln(P) + 0.9566 \quad (r^2 = 0.942)$$

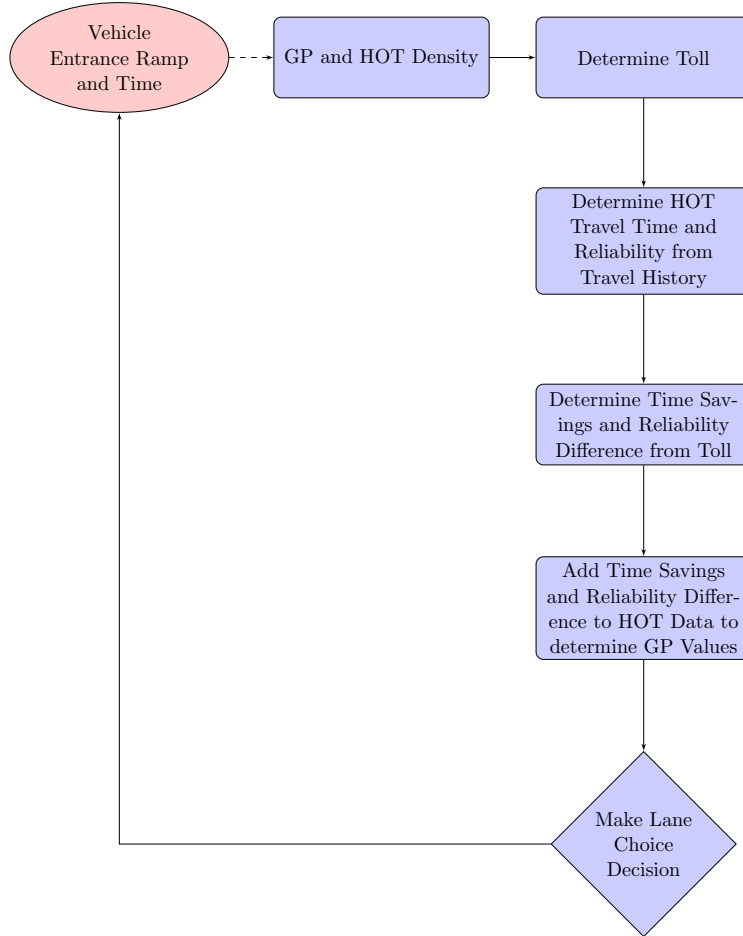
$$\Delta V_{offset} = 0.926 \ln(P) + 1.6636 \quad (r^2 = 0.9657)$$

where ΔV is time variance difference in minutes and P is price in USD

174 7.5 Calibration Process

175 The following flowchart displays the lane choice model calibration cycle using the grid search
 176 technique. Once lane choice decisions for all vehicles have been completed, the percentage of
 177 vehicles using the HOT lane ($Pr(L|R)$) is compared to the calibration target of 68.1%. The model
 178 coefficients are then adjusted to increase or decrease $Pr(L|R)$ and the process is repeated until the
 179 optimal coefficients are found.

Figure 3: Calibration Cycle



180 7.6 Resulting Coefficients

181 The lane choice parameters were for both congestion onset and offset. The resulting values are
 182 found in Table 4 below.

Table 4: Lane Choice Model Parameters for Calibration

Parameter	Carrion(2010)	Onset	Offset
Expected Travel Time	-0.672	-7.27	-10.7
Travel Time Variability	-0.228	-2.47	-3.63
HOT Lane Toll	-6.94	-6.94	-6.94
Alternative Specific Constant	-2.23	0	0

183 8 Testing of the Alternative Pricing Strategies

184 The calibrated HOT lane choice model was used to test the behavior of the alternative pricing
 185 strategies and how changing prices affect $Pr(L|R)$, which is the share of transponder owning
 186 SOVs which use the MnPASS lane.

187

$$Pr(L|R) = \frac{\# \text{ of transponder owning SOVs using the MnPASS lane(s)}}{\text{Total } \# \text{ of transponder SOVs using the corridor (all lanes)}} = Pr(L|R) \quad (8)$$

188 Each pricing strategies' coefficients were incrementally adjusted and the process rerun to determine
 189 the resulting $Pr(L|R)$. The average price and $Pr(L|R)$ were recorded for each iteration. The
 190 results were graphed and fit for each pricing strategy (congestion onset and offset). Table 5 displays
 191 the regression results from fitting one pricing strategy using a first, second, third and fourth order
 192 polynomial function. The fourth degree polynomial functions for each scenario are displayed in
 193 Table 6 and graphs of the Continuous Function (congestion onset and offset) are displayed in
 194 Figure 4.

Table 5: Continuous Pricing Function Onset Regression Results

Variable	Model 1 (1st order)	Model 2 (2nd order)	Model 3 (3rd order)	Model 4 (4th order)
Intercept	21.46(5.321)***	-0.9280(3.140)	-15.297(1.997)***	-25.884(0.9949)***
P	1.017(1.291)	35.019(2.892)***	71.931(3.546)***	108.91(2.670)***
P^2	-	-4.5576(0.3788)***	-17.218(1.129)***	-40.396(1.516)***
P^3	-	-	1.0781(0.09485)***	5.7446(0.2956)***
P^4	-	-	-	-0.2941(0.01849)***
n	44	44	44	44
r^2	0.0146	0.7825	0.9486	0.9931

(Standard error in parentheses)

Significance * 0.05, ** 0.01, *** 0.001

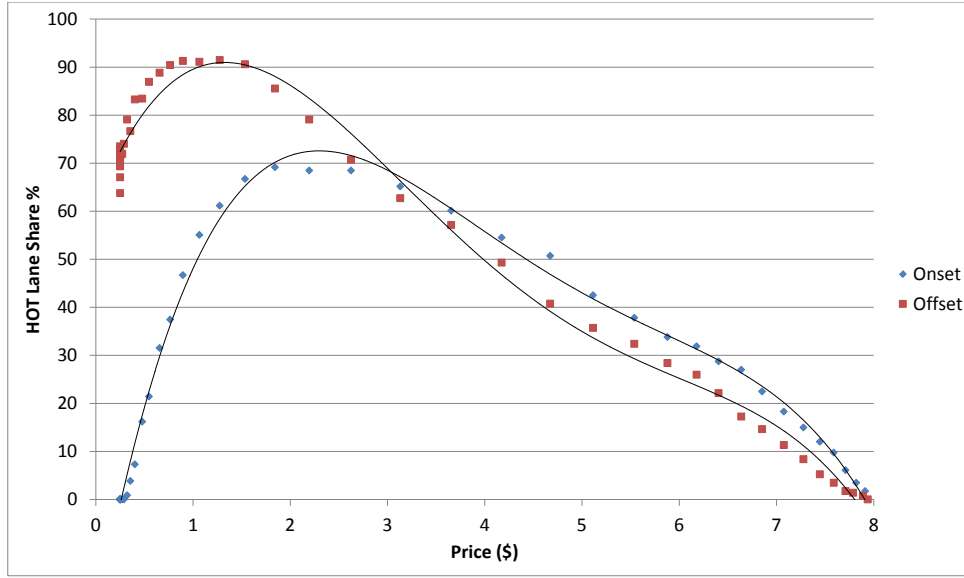
$Pr(L|R)$ is dependent variable, P is price in USD

Table 6: Pricing Function Model Equations

Pricing Function	Model	r^2
Onset		
<i>Continuous</i>	$Pr(L R) = -0.2941P^4 + 5.7446P^3 - 40.396P^2 + 108.91P - 25.884$	0.9931
<i>Unweighted</i>	$Pr(L R) = -0.1555P^4 + 3.6124P^3 - 31.812P^2 + 106.14P - 26.573$	0.9909
<i>HOT_{weighted}</i>	$Pr(L R) = -0.3468P^4 + 6.3111P^3 - 40.349P^2 + 98.579P - 22.116$	0.9493
<i>GP_{weighted}</i>	$Pr(L R) = -0.1785P^4 + 3.2471P^3 - 22.649P^2 + 66.301P - 13.515$	0.9604
Offset		
<i>Continuous</i>	$Pr(L R) = -0.2394P^4 + 4.4049P^3 - 27.423P^2 + 51.688P + 61.127$	0.9904
<i>UnweightedValue</i>	$Pr(L R) = -0.1284P^4 + 3.0066P^3 - 23.308P^2 + 51.99P + 61.762$	0.9887
<i>HOT_{weighted}</i>	$Pr(L R) = -0.1652P^4 + 2.9438P^3 - 17.877P^2 + 29.923P + 69.300$	0.9801
<i>GP_{weighted}</i>	$Pr(L R) = -0.0546P^4 + 1.2879P^3 - 10.691P^2 + 22.483P + 68.142$	0.9905

P is price in USD

Figure 4: Continuous Pricing Function



$$Pr(L|R) = -0.2941P^4 + 5.7446P^3 - 40.396P^2 + 108.91P - 25.884$$

$$r^2 = 0.9931$$

195 8.1 Elasticity

196 The functions above describe $Pr(L|R)$ as a function of toll price. The elasticity of $Pr(L|R)$ to
 197 price is determined by taking the derivative of the function and multiplying by the quotient of price

198 divided by $Pr(L|R)$.

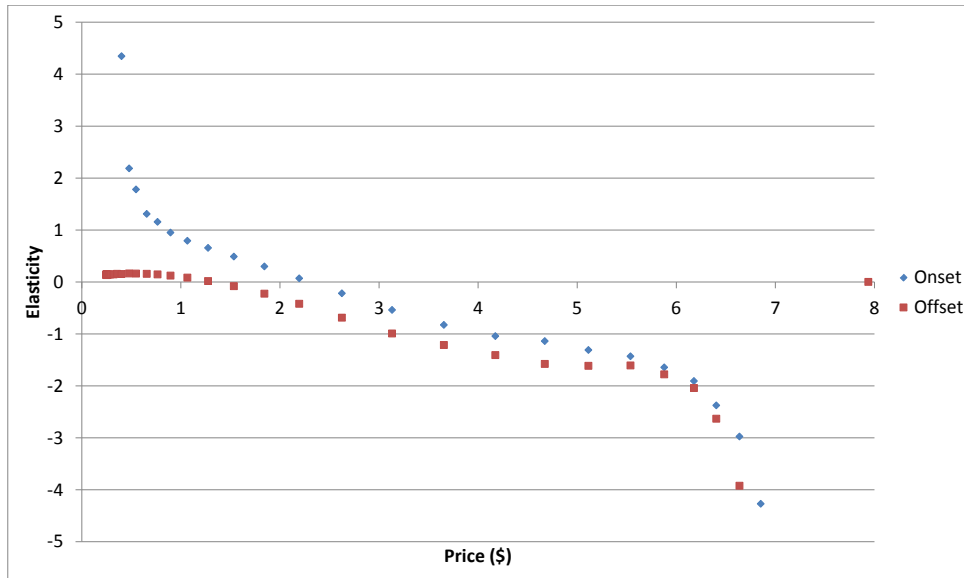
$$\varepsilon_{Pr(L|R)(P)} = \frac{P * Pr(L|R)'(P)}{Pr(L|R)(P)} = \frac{d \ln Pr(L|R)(P)}{d \ln P} \quad (9)$$

199

200

201 5 graphs elasticity as a function of price for the continuous function pricing strategy (onset and
 202 offset). The elasticity equations are displayed below each figure.

Figure 5: Continuous Pricing Function



$$\varepsilon_{Pr(L|R)(P)} = \frac{P * (-1.176 * 4 * P^3 + 17.23 * P^2 - 80.79 * P + 108.9)}{Pr(L|R)(P)}$$

$$\varepsilon_{Pr(L|R)(P)} = \frac{P * (-0.9576 * P^3 + 13.21 * P^2 - 54.85 * P + 51.69)}{Pr(L|R)(P)} \text{ where } p \text{ is price in USD}$$

203 9 Discussion

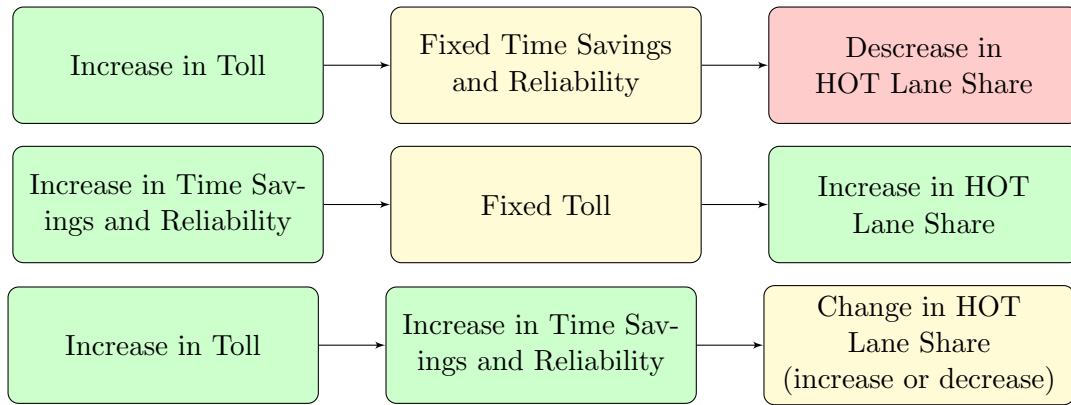
204 All four pricing strategies show a similar pattern in the relationship between $Pr(L|R)$ and price.
 205 The maximum $Pr(L|R)$ during congestion onset is achieved between \$2 and \$3, whereas during
 206 congestion offset, the greatest $Pr(L|R)$ occurs between \$1 and \$2. In general, the $Pr(L|R)$ during
 207 congestion offset is greater than during the onset due to the greater time savings and reliability
 208 per dollar toll price as demonstrated previously in 1 and 2. Table 7 shows the average price and
 209 $Pr(L|R)$ for each pricing strategy along with the standard deviation.

Table 7: Average $Pr(L|R)$ and Prices

Pricing Strategy	Avg Price (\$)	Std Dev Price (\$)	Avg $Pr(L R)$ (%)		Std Dev $Pr(L R)$ (%)	
			Onset	Offset	Onset	Offset
Continuous	2.93	2.93	54.6	24.4	31.6	24.7
Unweighted	3.19	3.20	54.1	24.5	36.9	32.6
HOT Weighted	3.65	2.93	49.4	24.5	31.6	19.3
GP Weighted	3.83	3.26	45.5	18.9	34.0	21.0

210 Figure 4 shows the rise and fall of the $Pr(L|R)$ as the toll increases (and therefore, time savings).
 211 When $Pr(L|R)$ reaches its maximum, elasticity switches from positive to negative. Figure 6
 212 outlines how changes in toll and time savings affect $Pr(L|R)$ and ultimately, elasticity to price.

Figure 6: Toll and Time Savings Effect on $Pr(L|R)$



213 At lower tolls, an increase in price results in a higher $Pr(L|R)$ (positive elasticity), whereas at
 214 higher tolls, an increase in price causes a decrease in $Pr(L|R)$ (negative elasticity). At lower tolls,
 215 the improved time savings and reliability outweigh the increase in toll. However, at higher tolls,
 216 the increase in toll outweighs greater time savings and reliability causing the $Pr(L|R)$ to decrease.

217 10 Conclusion

218 This paper outlined four HOT lane pricing strategies which could serve as alternatives to the
 219 current MnPASS pricing system. The current system relies on a series of density and price tables
 220 to determine the toll based strictly on HOT lane density. The proposed alternatives determine the
 221 toll based on a simple mathematical function relating HOT lane density (and GP density in three
 222 of the strategies) to price. The three value pricing strategies use the difference in GP and HOT lane
 223 density to determine the toll. Due to the nonlinear relationship between density and time savings,
 224 two of the strategies are weighted by either HOT density or GP density. The $HOT_{weighted}$ strategy
 225 combines the value pricing concept with the current algorithm's direct correlation between HOT
 226 density and price. For this reason, this pricing strategy would provide the greatest improvement

227 over the current pricing system while still maintaining some of the same logic. The continuous
228 function, on the other hand, most closely resembles the current pricing system, but fails to account
229 for the density in the GP lanes.

230 The behavior of the four alternative pricing strategies was tested using a fixed demand partial
231 equilibrium analysis. Using a calibrated lane choice model, simulated vehicles made decisions on
232 whether to use the MnPASS lane based on the toll and their anticipated time savings and improved
233 travel time reliability. The $Pr(L|R)$ was determined at various price increments for each pricing
234 system. These were plotted and fit with a fourth degree polynomial, the derivatives of which
235 correlate to the elasticity to price. In all cases, demand elasticity to price was positive at lower tolls
236 and negative at higher tolls. MnPASS users recognize the correlation between the toll price and
237 the time savings and travel time reliability provided by the lanes. The toll price acts as a proxy of
238 downstream congestion. At lower tolls, the travel time savings and reliability advantages outweigh
239 the cost of the toll and $Pr(L|R)$ rises. However, at higher tolls, the cost of using the lane begins
240 to outweigh the benefit and the $Pr(L|R)$ drops.

241 These results are estimated on a system where drivers have incomplete information about travel
242 time savings from HOT lane usage, and use price as a signal of time savings. In a context where
243 drivers were better informed (e.g. through Variable Message Signs or real-time congestion-aware
244 GPS navigation systems), results would likely be significantly different.

245 Future research should field test alternative pricing strategies and parameter values to identify
246 which best achieves the goals of maximizing use of the HOT lanes while maintaining reliable fre-
247 flowing speeds, recognizing that travelers may change their sensitivity to price if the relationship
248 between price and travel time savings changes.

249 Bibliography

- 250 91 Express Lanes (2013). Toll Schedule. <http://www.91expresslanes.com/schedules.asp>.
- 251 Carrion, C. (2010). *Value of Reliability: Actual Commute Experience Revealed Preference Approach*.
252 PhD thesis, University of Minnesota.
- 253 Carrion, C. and Levinson, D. (2012). Value of travel time reliability: A review of current evidence.
254 *Transportation research part A: policy and practice*, 46(4):720–741.
- 255 Colorado DOT (2013). I-25 HOV Express Lanes. [http://www.coloradodot.info/travel/
256 tolling/i-25-hov-express-lanes/rates-violations](http://www.coloradodot.info/travel/tolling/i-25-hov-express-lanes/rates-violations).
- 257 FasTrak (2013). I-15 FasTrak Tolls. <http://fastrak.511sd.com/i-15-fastrak-tolls>.
- 258 Florida DOT (2013). 95 Express. <http://www.95express.com/>.
- 259 Georgia State Road and Toll Authority (2013). Peach Pass. [http://peachpass.com/
260 peach-pass-toll-facilities/i-85-toll-rate-pricing](http://peachpass.com/peach-pass-toll-facilities/i-85-toll-rate-pricing).

- 261 Janson, M. and Levinson, D. (2014). Hot or not: Driver elasticity to price on the mnpass hot lanes.
262 *Research in Transportation Economics*, 44:21–32.
- 263 Katy Freeway Managed Lanes (2013). Toll Rate Schedule. [https://www.hctra.org/
264 katymanagedlanes/media/Katy_Toll_Sched.pdf](https://www.hctra.org/katymanagedlanes/media/Katy_Toll_Sched.pdf).
- 265 MnDOT (2013). MnPASS. <http://www.mnpass.org>.
- 266 Owen, A., Janson, M., and Levinson, D. (2013). Incremental Accessibility Benefits and HOT Lane
267 Subscription Choice. Technical report.
- 268 Transurban (USA) Operations Inc. (2013). 495 Express Lanes. [https://www.495expresslanes.
269 com/](https://www.495expresslanes.com/).
- 270 Washington Transportation Commission (2013). SR 167 HOT Lanes. [http://www.wstc.wa.gov/
271 HighwayTolling/SR167Rates/SR167HOTLanesWashingtonStateTransportationCommission.
272 htm](http://www.wstc.wa.gov/HighwayTolling/SR167Rates/SR167HOTLanesWashingtonStateTransportationCommission.htm).